



## SHORT COMMUNICATION

# Human Type II Taste Cells Express Angiotensin-Converting Enzyme 2 and Are Infected by Severe Acute Respiratory Syndrome Coronavirus 2 (SARS-CoV-2)



Máire E. Doyle, Ashley Appleton, Qing-Rong Liu, Qin Yao, Caio H. Mazucanti, and Josephine M. Egan

From the National Institute on Aging/Intramural Program, Baltimore, Maryland

Accepted for publication  
May 17, 2021.

Address correspondence to  
Josephine M. Egan, M.D., or  
Máire E. Doyle, Ph.D., National  
Institute on Aging/Intramural  
Program, 251 Bayview Blvd.,  
Baltimore, MD 21224. E-mail:  
[eganj@grc.nia.nih.gov](mailto:eganj@grc.nia.nih.gov) or  
[doyleme@nih.gov](mailto:doyleme@nih.gov).

Chemosensory changes are well-reported symptoms of severe acute respiratory syndrome coronavirus 2 (SARS-CoV-2) infection. The virus targets cells for entry by binding of its spike protein to cell-surface angiotensin-converting enzyme 2 (ACE2). It is not known whether ACE2 is expressed on taste receptor cells (TRCs), or whether TRCs are infected directly. *in situ* hybridization probe and an antibody specific to ACE2 indicated presence of ACE2 on a subpopulation of TRCs (namely, type II cells in taste buds in taste papillae). Fungiform papillae of a SARS-CoV-2<sup>+</sup> patient exhibiting symptoms of coronavirus disease 2019 (COVID-19), including taste changes, were biopsied. Presence of replicating SARS-CoV-2 in type II cells was verified by *in situ* hybridization. Therefore, taste type II cells provide a potential portal for viral entry that predicts vulnerabilities to SARS-CoV-2 in the oral cavity. The continuity and cell turnover of a patient's fungiform papillae taste stem cell layer were disrupted during infection and had not completely recovered 6 weeks after symptom onset. Another patient experiencing post-COVID-19 taste disturbances also had disrupted stem cells. These results demonstrate the possibility that novel and sudden taste changes, frequently reported in COVID-19, may be the result of direct infection of taste papillae by SARS-CoV-2. This may result in impaired taste receptor stem cell activity and suggest that further work is needed to understand the acute and postacute dynamics of viral kinetics in the human taste bud. (*Am J Pathol* 2021, 191: 1511–1519; <https://doi.org/10.1016/j.ajpath.2021.05.010>)

As many as 80% of people infected with severe acute respiratory syndrome coronavirus 2 (SARS-CoV-2) report taste and smell changes, as well as changes in overall oral sensitivity to commonly used condiments and spices.<sup>1</sup> The constellation of sensory symptoms can precede systemic symptoms, and therefore, has predictive value.<sup>2,3</sup> Interestingly, RNA for SARS-CoV-2 was detected in the submandibular glands and tumor of a patient undergoing tongue surgery for squamous carcinoma 2 days before the patient developed symptoms and had a positive nasal swab for the virus<sup>4</sup>; however, the taste tissue was not examined. The sensory symptoms need not be unitary as the virus can independently target all or any combination of the senses<sup>5,6</sup> and may even cause deficits or changes in a specific taste

quality. Branches of five cranial nerves [CNs; I (smell), V (chemesthesis: heat and pungency), and VII, IX, and X (taste) (Figure 1A)] are involved in relaying those specific senses to the central nervous system. Taste is first discriminated in taste receptor cells (TRCs) within the taste buds, which are autonomous organs primarily located in circumvallate papillae (CVP), foliate papillae, and fungiform papillae (FP) in the tongue. Each taste bud is supplied by nerve fibers, a capillary artery, and a vein. Solitary taste buds are buried in

Supported by the National Institute on Aging/NIH intramural research program project number 1ZIAAG000291-13 (J.M.E.); and an NIH Intramural Targeted Anti-COVID-19 (ITAC) Award (J.M.E.)

Disclosures: None declared.

the epithelial layer of the uvula, epiglottis, larynx, upper airways, and proximal esophagus. TRCs contain the machinery for discriminating five prototypic tastes that can be appreciated from commonly consumed foods: salty (pretzels), sweet (chocolate, sugar, and artificial sweeteners), bitter (coffee), umami (monosodium glutamate and sweet amino acids), and sour (citrus); one, more than one, or all, may be altered (dysgeusia) or absent (ageusia) because of SARS-CoV-2 infection.

Taste buds contain three distinct types of TRCs for mediating taste discrimination: type I (salty), type II (sweet, bitter, and umami; these are discriminated on the basis of specific receptor engagement on the cell surface while sharing downstream signal transduction mechanisms), and type III (sour) (Figure 1A).<sup>7,8</sup> Solitary chemosensory cells containing similar bitter receptors and signal transduction machinery, as are present in type II cells, reside in trachea, extrapulmonary bronchi, and the lung hilus, where, based on rodent investigations, they sense the microenvironment and regulate respiration rate through CN X. Bitter stimuli and cholinergic activation lead to decreased respiratory rates.<sup>9</sup> All taste buds have the same three TRC types, although ratios of cell types vary (Figure 1A). For example, type I cells are rare in FP.<sup>10</sup> TRCs are not neurons but are modified epithelial cells. Angiotensin-converting enzyme 2 (ACE2) expression has not been found in the neurons of the geniculate ganglion,<sup>11,12</sup> whose fibers innervate the FP via CN VII, or in sensory afferents of CN X<sup>13</sup> that innervate the solitary buds of the epiglottis, larynx, and chemosensory cells of the airways. In addition, CN V neurons, which mediate chemesthesis, do not express ACE2.<sup>14,15</sup> It therefore seemed unlikely that alterations in taste and chemesthesis are due to SARS-CoV-2 invasion of sensory afferents of four CNs, but more likely due to direct infection of the taste buds, lingual epithelium, and oral mucosa. Epithelial cells shed into saliva, the source of which could be lingual epithelium, salivary glands, and oral mucosal surfaces, from SARS-CoV-2–infected patients were recently reported to contain low ACE2 expression, and in some cases, viral RNA.<sup>16</sup> TRCs or chemosensory cells were not studied in that report. Herein, we demonstrate, using two highly specific techniques, *in situ* hybridization (ISH) probe and an antibody specific to ACE2, that ACE2 is present on a subpopulation of specialized TRCs [namely, phospholipase C  $\beta_2$  (PLC $\beta_2$ )-positive type II cells] in taste buds in taste papillae and that these type II cells are also infected with SARS-CoV-2.

## Materials and Methods

### Study Design, Study Population, and Setting

Human CVP tissue was obtained from cadaveric tongues and placed in formalin (National Disease Research Interchange, Philadelphia, PA) until processing at the National Institute on Aging (Baltimore, MD). Fresh human FP, eight or fewer per participant, were obtained with institutional review board approval (institutional review board/NIH

numbers 2018-AG-N010 and 2018-AG-N322) and with participants' written consent. All biopsies were performed in the Intramural Research Program (IRP) National Institute on Aging Clinical Research Unit. FP were excised after topical application of 1% lidocaine using sterile curved spring microscissors (McPherson-Vannas; WPI, Sarasota, FL) type number SR5603 (Roboz Surgical Instrument Co, Gaithersburg, MD). Individual papillae to be used for immunohistochemistry or ISH were immediately placed in 4% paraformaldehyde (Fisher Scientific, Atlanta, GA), cryoprotected with 20% sucrose (Millipore Sigma, St. Louis, MO) overnight at 4°C, frozen in OCT media (Tissue Tek O.C.T. Compound; Sakura Fintek, St. Torrance, CA), and stored at –80°C until use.

### Immunostaining of Human Lingual Tissue

CVP tissue and FP were cryosectioned (10  $\mu$ m thick) using a Leica CM 1950 cryostat (Leica, Buffalo Grove, IL), mounted onto ColorFrost Plus Micro slides (Fisher Scientific, Waltham, MA) and then stored at –80°C. Immunostaining was performed as described previously.<sup>10</sup> To permeabilize the cells in the tissue, slides were placed in Tris-buffered saline (TBS; pH 7.4; Quality Biologicals, Gaithersburg, MD) with 0.2% Triton-X 100 (Millipore Sigma) for 5 minutes at room temperature. They were then washed three times (2 minutes) in TBS. Antigen retrieval was performed by placing the slides in 10 mmol/L of sodium citrate buffer (pH 6.0; Vector Laboratories, Burlingame, CA) at 95°C for 30 minutes. The slides were left to cool at room temperature in the citrate buffer for a further 30 minutes and were then rinsed in water and then TBS as before. Sections were incubated with normal goat serum block consisting of 2% goat serum, 1% OmniPur BSA Fraction V (Millipore Sigma), 0.1% gelatin (Millipore Sigma), 0.1% Triton X-100 (Millipore Sigma), 0.05% Tween 20 (Millipore Sigma), and 0.05% sodium azide (Millipore Sigma) in TBS for 1 hour at room temperature. Sections were then incubated with primary antibodies (Table 1<sup>17–19</sup>) diluted in the same normal goat serum block at 4°C overnight. Tissue sections were rinsed with TBS with 5% Tween and incubated for 1 hour with fluorescently labeled secondary antibodies (Table 1) at 1:1000 dilution, then washed with TBS with 5% Tween. After nuclear staining (DAPI; Sigma Aldrich, St. Louis, MO), sections were mounted with Fluoromount G (Southern Biotechnology, Birmingham, AL). Controls used were incubation without primary antibody, isotype controls, and pre-absorption with a fivefold excess of the blocking peptide (ACE2). Appropriate no-primary-antibody controls were prepared with each individual batch of slides. Confocal fluorescence images were captured using Zen Black Lite software version 14 (Carl Zeiss AG, Oberlochen, Germany) on a Zeiss LSM-880 confocal microscope, and brightness and contrast were adjusted globally. All figures were compiled in Adobe Illustrator 2021 (San Jose, CA).

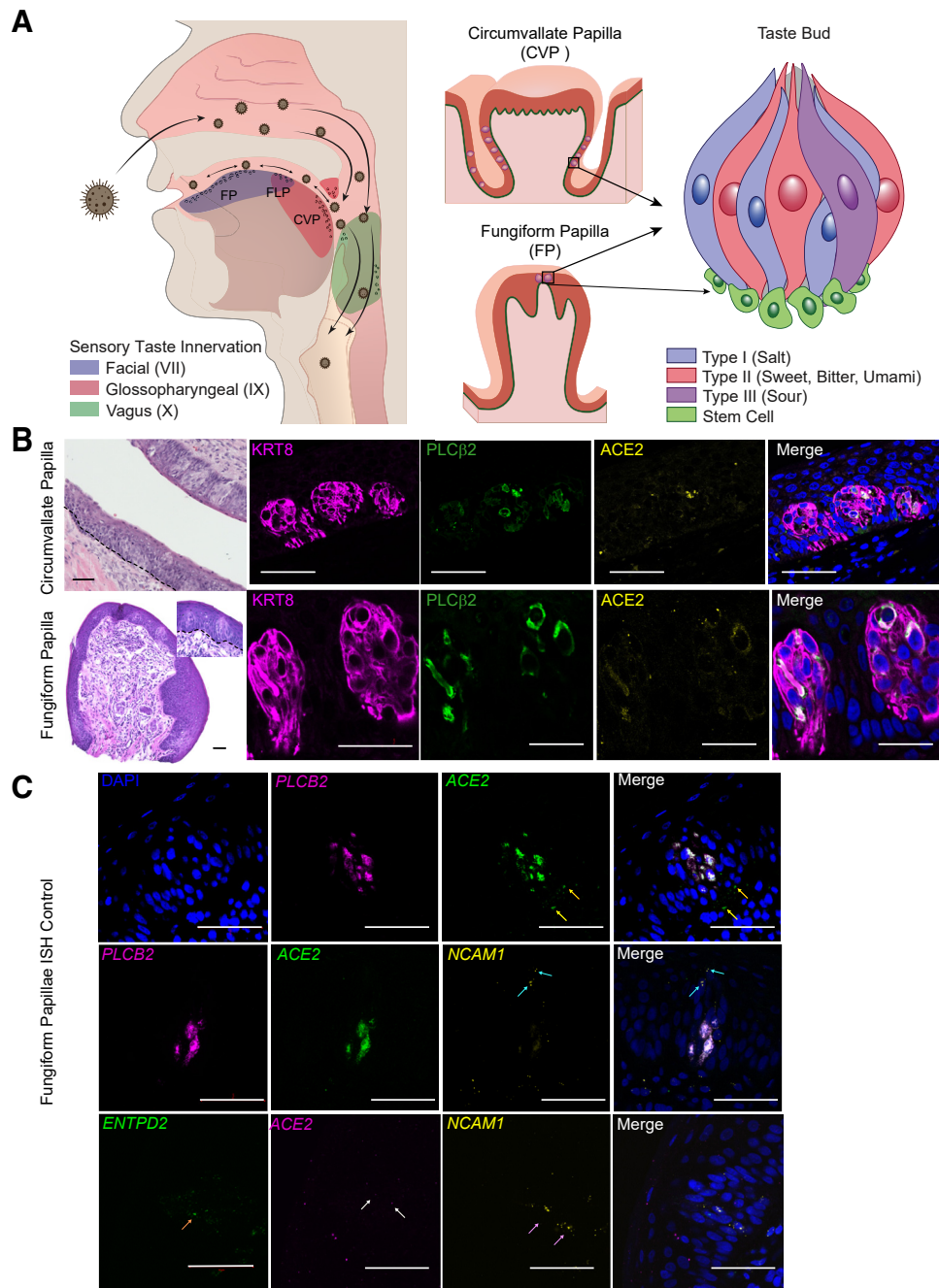


**Figure 1** The receptor for SARS-CoV-2 angiotensin-converting enzyme 2 (ACE2) is on type II taste bud cells in taste papillae of the tongue. **A:** The distribution of taste buds and chemosensory cells in the oropharyngeal cavity and how virus may infect the tongue and oropharyngeal areas. Branches of three cranial nerves (VII, IX, and X) are involved in relaying taste information to the central nervous system. Taste is first discriminated in taste receptor cells (TRCs) within taste buds located in circumvallate papillae (CVP), foliate papillae (FLP), and fungiform papillae (FP) in the tongue. Three defined TRCs relay five prototypic tastes. Stem cells immediately surrounding the taste bud receive signals from taste cells, prompting differentiation into a replacement TRC. Circles on tongue, uvula, epiglottis, and oropharyngeal areas represent taste buds and chemosensory cells. **Arrows** indicate the probable routes of viral entry on air eddies and flowing through and around (**double-headed arrows**) the oral cavity. **B:** Hematoxylin and eosin (H&E) staining and immunofluorescence staining (IFS) of CVP **top row** (post-mortem) and FP **bottom row** with taste buds embedded in the epithelial layer. Keratin 8 (KRT8) is a cytoskeletal marker of all TRCs, whereas phospholipase C  $\beta_2$  (PLC $\beta_2$ ) is an obligatory signal molecule in all type II cells. ACE2 and PLC $\beta_2$  were colocalized (merged signals) in IFS images. Nuclei are shown in blue, stained with DAPI. Likewise, H&E staining of a fresh FP with two taste buds (**inset**) and IFS for KRT8, PLC $\beta_2$ , and ACE2 show colocalization of the latter two proteins. **Dashed lines** in H&E of CVP and FP indicate the location of the line of stem cells. **C:** *In situ* hybridization (ISH) images of FP. **Top row:** Probes for PLCB2 and ACE2 confirm their colocalization in a fresh FP taste bud; nuclei are shown in blue. The **yellow arrows** indicate two areas outside the taste bud where ACE2 signal is found in the absence of PLCB2. **Middle row:** Colocalization of ACE2 and PLCB2 in the same cell is observed, and there is no overlap of the type III cell marker neural cell adhesion molecule 1 (NCAM1; **light blue arrows**)<sup>8</sup> with either of these two markers. **Bottom row:** No overlap of ACE2 (taste cell positivity indicated by two **white arrows**) with the probe for the transcript of the type I cell marker ectonucleoside triphosphate diphosphohydrolase 2 (ENTPD2; **orange arrow**)<sup>8</sup> and the type III marker NCAM1 (taste cell positivity indicated by two **pink arrows**). Scale bars = 50  $\mu$ m (**B** and **C**).

**Table 1** Primary and Secondary Antibodies Used, Their Dilutions, and Their RRID Numbers

Antigen	Source species	Dilution	Manufacturer; catalog no.; RRID
ACE2	Monoclonal mouse IgG <sub>2A</sub> clone number 171606	1:50	R&D Systems (Minneapolis, MN); MAB933; AB_2223153
KRT8	Rat	1:100	DSHB (University of Iowa, Iowa City, IA); TROMA-I; AB_531826
PLCβ <sub>2</sub>	Rabbit	1:100	Santa Cruz Biotechnology (Dallas, TX); sc-206; AB_632197
Anti-SARS-CoV-2 spike glycoprotein antibody	Mouse	1:100	Abcam (Cambridge, MA); ab272420; N/A <sup>17–19</sup>
Cleaved caspase-3	Rabbit	1:100	Millipore; ab3623; PA5-17869; AB_91556
Phosphorylated histone H3 (Ser10)	Rabbit	1:100	Invitrogen (Carlsbad, CA); PA5-17869; AB_10984484
Ki-67	Mouse	1:200	Agilent (Santa Clara, CA); M724029–2; AB_2250503
Rabbit IgG	Goat (AlexaFluor 488)	1:1000	Invitrogen; A27034; AB_2536097
Rabbit IgG	Goat (AlexaFluor 568)	1:1000	Invitrogen; A11036; AB_10563566
Mouse IgG2a	Goat (AlexaFluor 568)	1:1000	Invitrogen; A21134; AB_1500825
Rat IgG	Goat (AlexaFluor 647)	1:1000	Invitrogen; A21247; AB_141778
Mouse IgG	Goat (AlexaFluor 488)	1:1000	Invitrogen; A28175; AB_2536161

ACE2, angiotensin-converting enzyme 2; DSHB, Developmental Studies Hybridoma Bank; KRT8, keratin 8; N/A, not applicable; PLCβ<sub>2</sub>, phospholipase C β<sub>2</sub>; RRID, research resource identifier.

### RNAscope *in Situ* Hybridization

RNAscope probes were all obtained from Advanced Cell Diagnostics (Newark, CA) (Table 2). V-nCoV2019-S (catalog number 848561) is an antisense probe specific to the viral genomic positive strand RNA of the spike protein sequence, and V-nCoV2019-orf1ab (catalog number 859151) is a sense probe specific to the viral open reading frame 1 ab (ORF1ab) negative strand RNA produced when the virus is replicating.<sup>20</sup> Taste receptor cell marker probe for type I cell was *ENTPD2* (catalog number 507941); for type II cell, *PCLB2* (custom designed); and for type III cell, *NCAM1* (catalog number 421468). *ENTPD2* is translated into ectonucleoside triphosphate diphosphohydrolase 2, which is expressed only on type I cells,<sup>21</sup> whereas *NCAM1* is translated to a neural cell adhesion molecule that is a cell surface marker for type III cells.<sup>22</sup> FP were sectioned at 10 μm using RNase-free conditions on a Leica CM 1950 cryostat, mounted onto ColorFrost Plus Micro (Fisher Scientific) slides, and stored at –80°C in a slide box that was placed in a sealed Ziploc bag until use. Retrieving mRNA targets from the fixed frozen FP sections, pretreatment,

probe hybridizations, and labeling were all performed according to RNAscope Multiplex Fluorescent Detection Kit version 2 (catalog number 323100) protocol: the negative control probe was a universal control probe targeting the bacterial *Dapb* gene (<https://www.ncbi.nlm.nih.gov/nucleotide>; accession number EF191515) from the *Bacillus subtilis* strain (catalog number 320871). Positive controls were probes to the human transcripts *POLR2A* (C1) and *PIIB* (C2), and *UBC* (C3; catalog number 320861) was used for RNAscope Multiplex Fluorescent Assay. Images were acquired using Zen software on a Zeiss LSM 880 confocal microscope.

### Quantification of Percentages of Proliferating Cells

The numbers of cells positive for Ki-67 and phosphorylated histone H3 (PHH3) were determined using the Cytonuclear FL algorithm in the HALO image analysis software platform (HALO platform 2.2; Indica Labs, Albuquerque, NM) that identified Ki-67–positive nuclei (green), PHH3–positive nuclei (red), and DAPI-stained nuclei (blue) on

**Table 2** RNAscope ISH Probes

Gene symbol	ISH probe	Catalog no.	Accession no.	ZZ probe pairs	Nucleotide position
SARS-CoV-2 (S)	V-nCoV2019-S <sup>20</sup>	848561-C1	NC_045512.2	20	21,631–23,303
SARS-CoV-2 (ORF1ab)	V-nCoV2019-orf1ab-sense <sup>20</sup>	859151-C2	NC_045512.2	40	1583–4388
<i>ACE2</i>	Probe-Hs-ACE2	848151-C1	NM_021804.3	20	307–1267
<i>PLCB2</i>	Probe-Hs-PCLB2	Custom-C3	NM_004573.3	13	3822–4621
<i>ENTPD2</i>	Probe-Hs-ENTPD2	507941-C1	NM_203468.2	20	161–1473
<i>NCAM1</i>	Probe-Hs-NCAM1	421468-C2	NM_001242608.1	20	832–1751

All probes used were off the shelf from Advanced Cell Diagnostics, with the exception of *PLCB2*, which was designed in house. The website used to obtain the NM accession numbers was <https://www.ncbi.nlm.nih.gov/nucleotide>.

ISH, *in situ* hybridization.

immunostained sections imaged on the LSM 880 using the 20× objective. The percentage of Ki-67–positive cells was determined as a percentage of the total number of DAPI-positive nuclei. The percentage of Ki-67–positive cells positive for the mitotic marker PHH3 was also determined. Cells in three to four sections from each of two FP per individual were counted. One-way analysis of variance with the Tukey multiple comparison was performed using GraphPad Prism 9 (GraphPad Software Inc., San Diego, CA). The data are presented as means ± SEM, and  $P < 0.05$  is considered statistically significant.

## Results

Humans have approximately 5000 to 10,000 taste buds, of which about half are buried on the sides of CVP (Figure 1, A and B).<sup>23</sup> ACE2 in taste buds within CVP of post-mortem tissue was investigated by immunofluorescence staining (IFS) and found to be co-expressed with PLCβ<sub>2</sub>, a marker and obligatory signal transduction molecule in type II TRCs (Figure 1B).<sup>24</sup> Taste buds within foliate papillae, which are vertical folds on the sides of the tongue, were not sufficiently preserved for definitive ACE2 IFS. Obtaining fresh FP, on the other hand, is a relatively simple biopsy procedure. There are 150 to 200 FP on the front half of the tongue, and each FP contains zero to two buds on its surface (Figure 1B). TRCs are replaced approximately every 14 days by replicating stem cells underneath the epithelial layer of FP.<sup>25</sup> ACE2 was found to be present in TRCs within taste buds of freshly biopsied FP, where it colocalized with PLCβ<sub>2</sub> by IFS (Figure 1B). This was confirmed by ISH (Figure 1C); ACE2 was present in the area outside of the taste bud. It therefore seems evident that taste buds provide a potential portal for SARS-CoV-2 entry. ACE2 was not found to be co-expressed with type I and III cell markers (ISH) (Figure 1C).

Participant 114 (female with controlled hypertension, 45 years old) in the study contracted SARS-CoV-2 (SARS-CoV-2<sup>+</sup> by PCR), and she reported changes in sweet taste (chocolate did not taste like chocolate) and in chemesthesis (a curry meal tasted white) beginning 15 days prior. Her tongue had enlarged, red-appearing FP, in contrast with the shiny FP 3 months later (Figure 2A). Four FP were removed for histology. Of these four, just one contained taste buds (Figure 2B). An RNAscope antisense probe specific to the genomic positive strand RNA (for proof of viral infection) of the spike protein (*S*) sequence of SARS-CoV-2 and a sense probe specific to the *ORF1ab* negative strand RNA (for proof of viral replication) indicated the presence of replicating SARS-CoV-2 in *PLCB2*-positive cells (Participant 114) (Figure 2C). Note the arrow pointing to another viral-positive cell in the neighboring taste bud. A sex- and age-matched control FP was negative for the virus (Supplemental Figure S1A). The virus was present in lamina propria of Participant 114 by both ISH and IFS

(Supplemental Figure S1, B and C). The stem cell layer within the FP of Participant 114 had disruptions based on immunostaining for Ki-67 (a marker of cell turnover). It had improved on a subsequent biopsy 6 weeks later, by which time her sense of taste had recovered (Figure 2D). An age- and sex-matched control was used as a healthy control for Participant 114. Participant 089 (male with no preexisting medical conditions, 63 years old) first donated FP in 2019 (pre-SARS-CoV-2). He was biopsied 6 weeks after being SARS-CoV-2<sup>+</sup> by PCR but at a time when he still had mild dysgeusia. Specifically, his sweet (chocolate was almost tasteless) and bitter (coffee tasted like mud) sensations were still impaired by history. At this time, his other viral symptoms (namely, chills, muscle aches, joint pain, and brain fog) had abated, and he had returned to work. He was biopsied again at 10 weeks after SARS-CoV-2. No virus was present in his FP (Supplemental Figure S1D); however, his stem cell layer had disruptions 6 weeks after infection compared with that in 2019, and the disruptions were less obvious and taste perception was recovering (coffee was now perceived as tasteless, but not muddy) at 10 weeks (Figure 2D). The total number of cells positive for Ki-67 (as a percentage of DAPI-positive nuclei) and the percentage of Ki-67 cells positive for the mitotic marker PHH3 in three to four sections from each of two FP from participants at the three time points shown in Figure 2D were counted (Figure 2E). One-way analysis of variance showed that the percentage of Ki-67–positive cells in FP of Participant 114 (during) was significantly lower than those in sections taken from the healthy, sex- and age-matched control and 6 weeks after coronavirus disease 2019 (COVID-19) ( $P < 0.0001$ ). The percentage values of Ki-67–positive cells in FP of Participant 089 at 6 and 10 weeks after COVID-19 were lower than those of his pre-COVID-19 value ( $P < 0.01$  for 6 weeks after versus before). The percentage of PHH3/Ki-67–positive cells in the FP sections from Participant 114 during COVID-19 was significantly lower than those of the control ( $P < 0.0001$ ) and Participant 114 at 6 weeks after COVID-19 ( $P < 0.01$ ). The percentages of PHH3/Ki-67–positive cells in FP sections from Participant 089 at 6 and 10 weeks after COVID-19 were significantly lower than those of the pre-COVID-19 FP sample ( $P < 0.001$  and  $P < 0.05$ , respectively). A marker of cellular apoptosis, cleaved caspase 3, was not expressed in the stem cell layer during COVID-19 in Participant 114 or during the period of taste dysfunction of Participant 089 (Figure 2F).

## Discussion

Oral infection and replication with SARS-CoV-2 occurred in taste bud type II cells. Virus may be transported to the oral cavity on air eddies containing virus in droplets directly into mouth and/or in droplets, nasal mucous, or epithelial cells shed from the nose (Figure 1A). Although SARS-CoV-2 infection is noted in oral cavity, salivary glands, gingiva,

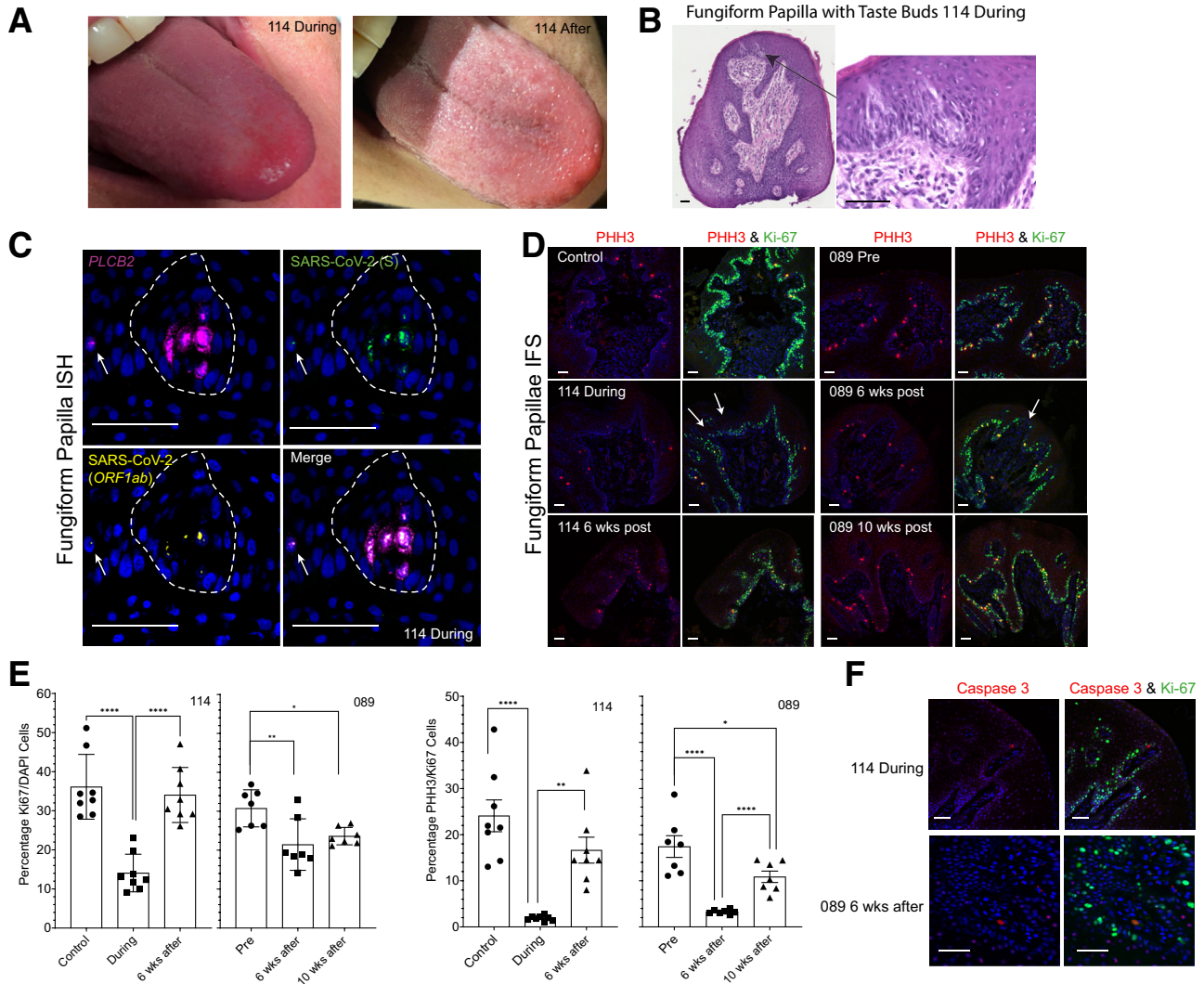


**Figure 2** Evidence of SARS-CoV-2 in human fungiform papillae (FP). **A:** Tongue images of Patient 114 moments before biopsy of her FP during the course of COVID-19 and 3 months later. **B:** Hematoxylin and eosin staining of a section through the FP from Patient 114 that contained two taste buds; the consecutive section was used for *in situ* hybridization (ISH), outlining the presence of viral particle (SARS-CoV-2 S) probe for the spike mRNA and the SARS-CoV-2 (*ORF1ab*) probe for the replicating virus, shown in Figure 2C. **C:** An antisense probe specific to the genomic positive strand RNA of the spike protein (S) sequence of SARS-CoV-2 and a sense probe to the SARS-CoV-2 *ORF1ab* negative strand RNA indicate the presence of replicating virus in *PLCB2*-positive cells (Participant 114). Taste bud is outlined by white dashed lines. Note the arrow pointing to another viral positive cell in the neighboring taste bud. **D:** The proliferation of the stem cell layer of the FP by immunostaining for the marker of all active phases of cell cycle Ki-67 and the late G<sub>2</sub> and M phase marker phosphorylated histone H3 (PHH3). **Left columns:** An FP from an age- and sex-matched control participant for Participant 114 compared with during and after SARS-CoV-2 infection. **White arrows** indicate the breaks in the otherwise continuous layer of stem cells. **Right columns:** A continuous stem cell layer in Participant 089 before, but multiple breaks especially at 6 weeks, and less at 10 weeks, after SARS-CoV-2. **E:** The percentages of total cells (as determined by DAPI-stained nuclei) positive for Ki-67 and the percentage of Ki-67-positive cells that are also positive for PHH3. **F:** The proliferating taste stem cells do not express cleaved caspase 3. Data are given as means ± SEM (E). \**P* < 0.05, \*\**P* < 0.01, and \*\*\*\**P* < 0.0001. Scale bars = 50 μm (B–D and F). IFS, immunofluorescence staining.

oral mucosa, and saliva,<sup>16</sup> there has been no publication on taste tissue as of yet. Furthermore, previous studies<sup>16,26,27</sup> did not address the cellular location of ACE2 within human taste buds using the highly specific techniques of ISH (mRNA) and IFS (protein). Taste buds do not contain a resident adaptive immune system,<sup>28</sup> and TRCs account for all cells within taste buds. In contrast to SARS-CoV-2 infection in the olfactory system,<sup>29</sup> where it is the

sustentacular cells that are affected, our data show evidence for infection in the taste apparatus per se (ie, the taste buds). Replication of virus can likely then occur undisturbed and allow for transmission from the taste bud into circulation, and locally infect lingual and salivary gland epithelium, oral mucosa, larynx, and even the lungs. TRCs within taste buds contain interferon receptors, and a systemic response to virus should eliminate the virus while simultaneously

leading to taste changes.<sup>28</sup> Although not investigated directly, it is possible that there could be indirect effects on the neuronal<sup>30</sup> or blood supply to the taste buds, as is noted by the detection of ACE2 in the proximity of the taste buds. We further propose that deficient stem cell turnover will result in TRCs not being effectively replaced and that this explains why some people have slow recovery of their complete taste repertoire. The detection of actively replicating SARS-CoV-2 in *PLCB2*-containing cells indicates that the virus has a direct route into TRCs via ACE2 on the type II cells.

Direct infection of type II cells does not explain why tastes not transduced by type II cells (ie, salt and sour) are affected during COVID-19. One possibility is infection by mechanisms independent of membrane-bound ACE2. ADAM metallopeptidase domain 17 (ADAM17) cleaves ACE2, resulting in shedding of a soluble ACE2.<sup>31</sup> Binding of SARS-CoV-2 has been shown to increase shedding of ACE2. This would be permissive to virus in the oral and taste bud milieu to bind to soluble ACE2 that is then picked up by type I and III cells. A second mechanism involves the virus itself promoting the production of casein kinase II (CK2)-containing filopodial protrusions that the virus then uses to enter adjacent cells.<sup>32</sup> This could be especially true of type I cells as they wrap around type II cells.<sup>33</sup> Both mechanisms could explain an infection-mediated loss of or aberrant salt and sour taste perception. Although we observe SARS-CoV-2 by both ISH and IFS in the lamina propria, likely associated with blood vessels, it is probable that any virus in the overlying mucosa, as was seen by Huang et al,<sup>16</sup> had cleared by day 14 of infection, the time point at which the biopsy was taken.

The presence of ACE2 on type II cells specifically is particularly intriguing because these cells taste amino acids, and ACE2 in the gut has been shown to dimerize with amino acid transporters, where it plays a vital role in efficient amino acid absorption.<sup>34</sup> We hypothesize that ACE2 is also present on the chemosensory cells present in airways as their cellular machinery is similar to type II cells in taste buds. They contain bitter receptors activated by ligands, such as cycloheximide, a bitter receptor agonist, and require PLC $\beta_2$  for signal transduction.<sup>9</sup> Therefore, viral infection of those cells might directly decrease respiratory drive, resulting in worsening oxygen desaturation. The role of chemosensory cells in the upper airways or of TRCs in taste buds during SARS-CoV-2 infection has not been studied because of practical difficulties: obtaining a fresh CVP, where numerous taste buds reside and where they are larger than in FP, is not a viable option because CVPs have not been shown to regrow<sup>35</sup>; obtaining FP or especially fresh tissue from airways in sick people has associated medical conundrums; there is a paucity of taste buds within FP as there are at most two taste buds but sometimes just one and occasionally none, even in young people<sup>36</sup>; taste buds may be damaged by virus and not be recognizable, especially to an untrained eye; taste buds are buried in the epithelial layer,

where they occupy <1% of the total mass of a papilla (Figure 1, A and B), and therefore are easily missed if the whole papilla is not systematically sectioned. Finally, even when present, a taste bud in an FP is approximately 30  $\mu$ m in diameter, thereby providing a maximum of three to four slides with taste bud cells for in-depth investigation. This had led to the weakness of the study: we had one FP containing taste buds from one participant in which to study the acute effects of the virus.

In conclusion, colocalization of SARS-CoV-2 virus, type II taste cell marker, and the viral receptor ACE2 provides evidence for replication of this virus within taste buds that could account for acute taste changes during active COVID-19. This work also shows that proliferation of the taste stem cells in recovering patients may take weeks to return to their pre-COVID-19 state, providing a hypothesis for more chronic disruption of taste sensation, reports of which are now appearing in the medical literature.<sup>37–42</sup> It is worthwhile noting that the influenza A virus subtype H3N2 that caused the pandemic of 1968 to 1969 resulted in long-term alternations of taste and smell in some patients. Patients experiencing postinfluenza hypogeusia and dysgeusia many years after their infection had disrupted taste bud architecture with decreased numbers of TRCs and were lacking cilia in the pore region of the taste bud.<sup>43</sup>

## Acknowledgments

We thank all the participants of the study (2018-AG-N010) and all the Intramural Research Program (IRP) National Institute on Aging clinical staff.

## Supplemental Data

Supplemental material for this article can be found at <http://doi.org/10.1016/j.ajpath.2021.05.010>.

## References

1. Lechien JR, Chiesa-Estomba CM, Beckers E, Mustin V, Ducarme M, Journe F, Marchant A, Jouffe L, Barillari MR, Cammaroto G, Ciciu MP, Hans S, Saussez S: Prevalence and 6-month recovery of olfactory dysfunction: a multicentre study of 1363 COVID-19 patients. *J Intern Med* 2021, 451–461
2. Menni C, Valdes AM, Freidin MB, Sudre CH, Nguyen LH, Drew DA, Ganesh S, Varsavsky T, Cardoso MJ, El-Sayed Moustafa JS, Visconti A, Hysi P, Bowyer RCE, Mangino M, Falchi M, Wolf J, Ourselein S, Chan AT, Steves CJ, Spector TD: Real-time tracking of self-reported symptoms to predict potential COVID-19. *Nat Med* 2020, 26:1037–1040
3. Melley LE, Bress E, Polan E: Hypogeusia as the initial presenting symptom of COVID-19. *BMJ Case Reports* 2020, 13:e236080
4. Guerini-Rocco E, Taormina SV, Vacirca D, Ranghiero A, Rappa A, Fumagalli C, Maffini F, Rampinelli C, Galetta D, Tagliabue M, Ansarin M, Barberis M: SARS-CoV-2 detection in formalin-fixed paraffin-embedded tissue specimens from surgical resection of tongue squamous cell carcinoma. *J Clin Pathol* 2020, 73:754–757

5. Adamczyk K, Herman M, Fraczek J, Piec R, Szykula-Piec B, Zaczynski A, Wojtowicz R, Bojanowski K, Rusyan E, Krol Z, Wierzba W, Franek E: Sensitivity and specificity of prediction models based on gustatory disorders in diagnosing COVID-19 patients: a case-control study. *medRxiv* 2020, [Preprint] doi:10.1101/2020.05.31.20118380
6. Parma V, Ohla K, Veldhuizen MG, Niv MY, Kelly CE, Bakke AJ, et al: More than smell-COVID-19 is associated with severe impairment of smell, taste, and chemesthesis. *Chem Senses* 2020, 45: 609–622
7. Kinnamon SC, Finger TE: Recent advances in taste transduction and signaling. *F1000Research* 2019, 8. F1000 Faculty Rev-2117
8. Roper SD, Chaudhari N: Taste buds: cells, signals and synapses. *Nat Rev Neurosci* 2017, 18:485–497
9. Krasteva G, Canning BJ, Hartmann P, Veres TZ, Papadakis T, Mühlfeld C, Schliecker K, Tallini YN, Braun A, Hackstein H, Baal N, Weihe E, Schütz B, Kotlikoff M, Ibanez-Tallon I, Kummer W: Cholinergic chemosensory cells in the trachea regulate breathing. *Proc Natl Acad Sci U S A* 2011, 108:9478–9483
10. Doyle ME, Fiori JL, Gonzalez Mariscal I, Liu QR, Goodstein E, Yang H, Shin YK, Santa-Cruz Calvo S, Indig FE, Egan JM: Insulin is transcribed and translated in mammalian taste bud cells. *Endocrinology* 2018, 159:3331–3339
11. Dvoryanchikov G, Hernandez D, Roebber JK, Hill DL, Roper SD, Chaudhari N: Transcriptomes and neurotransmitter profiles of classes of gustatory and somatosensory neurons in the geniculate ganglion. *Nat Commun* 2017, 8:760
12. Zhang J, Jin H, Zhang W, Ding C, O’Keeffe S, Ye M, Zuker CS: Sour sensing from the tongue to the brain. *Cell* 2019, 179:392–402.e15
13. Prescott SL, Umans BD, Williams EK, Brust RD, Liberles SD: An airway protection program revealed by sweeping genetic control of vagal afferents. *Cell* 2020, 181:574–589.e14
14. Nguyen MQ, Le Pichon CE, Ryba N: Stereotyped transcriptomic transformation of somatosensory neurons in response to injury. *Elife* 2019, 8:e49679
15. Nguyen MQ, Wu Y, Bonilla LS, von Buchholtz LJ, Ryba NJP: Diversity amongst trigeminal neurons revealed by high throughput single cell sequencing. *PLoS One* 2017, 12:e0185543
16. Huang N, Pérez P, Kato T, Mikami Y, Okuda K, Gilmore RC, et al: SARS-CoV-2 infection of the oral cavity and saliva. *Nat Med* 2021, 27:892–903
17. Puelles VG, Lütgehetmann M, Lindenmeyer MT, Sperhake JP, Wong MN, Allweiss L, Chilla S, Heinemann A, Wanner N, Liu S, Braun F, Lu S, Pfefferle S, Schröder AS, Edler C, Gross O, Glatzel M, Wichmann D, Wiech T, Kluge S, Pueschel K, Aepfelbacher M, Huber TB: Multiorgan and renal tropism of SARS-CoV-2. *N Engl J Med* 2020, 383:590–592
18. Yang AC, Kern F, Losada PM, Maat CA, Schmartz G, Fehlmann T, Schaum N, Lee DP, Calcuttawala K, Vest RT, Gate D, Berdnik D, McNERney MW, Channappa D, Cobos I, Ludwig N, Schulz-Schaeffer WJ, Keller A, Wyss-Coray T: Dysregulation of brain and choroid plexus cell types in severe COVID-19. *Nature* 2021, 595: 565–571
19. Meinhardt J, Radke J, Dittmayer C, Mothes R, Franz J, Laue M, Schneider J, Brünink S, Hassan O, Stenzel W, Windgassen M, Rößler L, Goebel H-H, Martin H, Nitsche A, Schulz-Schaeffer WJ, Hakroush S, Winkler MS, Tampe B, Elezskurtaj S, Horst D, Oesterhelweg L, Tsokos M, Heppner BI, Stadelmann C, Drosten C, Corman VM, Radbruch H, Heppner FL: Olfactory transmucosal SARS-CoV-2 invasion as part of central nervous system entry in COVID-19 patients. *Nat Neurosci* 2021, 24:168–175
20. Liu J, Babka AM, Kearney BJ, Radoshitzky SR, Kuhn JH, Zeng X: Molecular detection of SARS-CoV-2 in formalin-fixed, paraffin-embedded specimens. *JCI Insight* 2020, 5:e139042
21. Vandenbeuch A, Anderson CB, Parnes J, Enjoji K, Robson SC, Finger TE, Kinnamon SC: Role of the ectonucleotidase NTPDase2 in taste bud function. *Proc Natl Acad Sci U S A* 2013, 110:14789–14794
22. Takagi H, Seta Y, Kataoka S, Nakatomi M, Toyono T, Kawamoto T: Mash1-expressing cells could differentiate to type III cells in adult mouse taste buds. *Anat Sci Int* 2018, 93:422–429
23. Witt M: Anatomy and development of the human taste system. *Handb Clin Neurol* 2019, 164:147–171
24. Rössler P, Boekhoff I, Tareilus E, Beck S, Breer H, Freitag J: G protein betagamma complexes in circumvallate taste cells involved in bitter transduction. *Chem Senses* 2000, 25:413–421
25. Perea-Martinez I, Nagai T, Chaudhari N: Functional cell types in taste buds have distinct longevities. *PLoS One* 2013, 8:e53399
26. Zhong M, Lin B, Pathak JL, Gao H, Young AJ, Wang X, Liu C, Wu K, Liu M, Chen JM, Huang J, Lee LH, Qi CL, Ge L, Wang L: ACE2 and furin expressions in oral epithelial cells possibly facilitate COVID-19 infection via respiratory and fecal-oral routes. *Front Med* 2020, 7: 580796
27. Sakaguchi W, Kubota N, Shimizu T, Saruta J, Fuchida S, Kawata A, Yamamoto Y, Sugimoto M, Yakeishi M, Tsukinoki K: Existence of SARS-CoV-2 entry molecules in the oral cavity. *Int J Mol Sci* 2020, 21:6000
28. Mazucanti CH, Egan JM: SARS-CoV-2 disease severity and diabetes: why the connection and what is to be done? *Immun Ageing A* 2020, 17:21
29. Brann DH, Tsukahara T, Weinreb C, Lipovsek M, Van den Berge K, Gong B, Chance R, Macaulay IC, Chou HJ, Fletcher RB, Das D, Street K, de Bezieux HR, Choi YG, Rizzo D, Dudoit S, Purdom E, Mill J, Hachem RA, Matsunami H, Logan DW, Goldstein BJ, Grubb MS, Ngai J, Datta SR: Non-neuronal expression of SARS-CoV-2 entry genes in the olfactory system suggests mechanisms underlying COVID-19-associated anosmia. *Sci Adv* 2020, 6: eabc5801
30. Ismail II, Gad KA: Absent blood oxygen level-dependent functional magnetic resonance imaging activation of the orbitofrontal cortex in a patient with persistent cacosmia and cacogeusia after COVID-19 infection. *JAMA Neurol* 2021, 78:609–610
31. Heurich A, Hofmann-Winkler H, Gierer S, Liepold T, Jahn O, Pöhlmann S: TMPRSS2 and ADAM17 cleave ACE2 differentially and only proteolysis by TMPRSS2 augments entry driven by the severe acute respiratory syndrome coronavirus spike protein. *J Virol* 2014, 88:1293–1307
32. Bouhaddou M, Memon D, Meyer B, White KM, Rezelj VV, Correa Marrero M, et al: The global phosphorylation landscape of SARS-CoV-2 infection. *Cell* 2020, 182:685–712.e19
33. Calvo SS, Egan JM: The endocrinology of taste receptors. *Nat Rev Endocrinol* 2015, 11:213–227
34. Camargo SMR, Vuille-Dit-Bille RN, Meier CF, Verrey F: ACE2 and gut amino acid transport. *Clin Sci (Lond)* 2020, 134: 2823–2833
35. Ferrell F, Tsuetaki T: Regeneration of taste buds after surgical excision of human vallate papilla. *Exp Neurol* 1984, 83:429–435
36. Arvidson K, Cottler-Fox M, Friberg U: Fine structure of taste buds in the human fungiform papilla. *Scand J Dent Res* 1981, 89: 297–306
37. Nalbandian A, Sehgal K, Gupta A, Madhavan MV, McGroder C, Stevens JS, Cook JR, Nordvig AS, Shalev D, Sehrawat TS, Ahluwalia N, Bikdeli B, Dietz D, Der-Nigoghossian C, Liyanage-Don N, Rosner GF, Bernstein EJ, Mohan S, Beckley AA, Seres DS, Choueiri TK, Uriel N, Ausiello JC, Accili D, Freedberg DE, Baldwin M, Schwartz A, Brodie D, Garcia CK, Elkind MSV, Connors JM, Bilezikian JP, Landry DW, Wan EY: Post-acute COVID-19 syndrome. *Nat Med* 2021, 27:601–615
38. Carfi A, Bernabei R, Landi F: Persistent symptoms in patients after acute COVID-19. *JAMA* 2020, 324:603–605
39. Carvalho-Schneider C, Laurent E, Lemaigen A, Beaufile E, Bourbao-Tournois C, Laribi S, Flament T, Ferreira-Maldent N, Bruyère F, Stefic K, Gaudy-Graffin C, Grammatico-Guillon L, Bernard L: Follow-up of adults with noncritical COVID-19 two months after symptom onset. *Clin Microbiol Infect* 2021, 27:258–263

40. Chopra V, Flanders SA, O'Malley M, Malani AN, Prescott HC: Sixty-day outcomes among patients hospitalized with COVID-19. *Ann Intern Med* 2021, 174:576–578
41. Arnold DT, Hamilton FW, Milne A, Morley AJ, Viner J, Attwood M, Noel A, Gunning S, Hatrick J, Hamilton S, Elvers KT, Hyams C, Bibby A, Moran E, Adamali HI, Dodd JW, Maskell NA, Barratt SL: Patient outcomes after hospitalisation with COVID-19 and implications for follow-up: results from a prospective UK cohort. *Thorax* 2021, 76:399–401
42. Moreno-Pérez O, Merino E, Leon-Ramirez JM, Andres M, Ramos JM, Arenas-Jiménez J, Asensio S, Sanchez R, Ruiz-Torregrosa P, Galan I, Scholz A, Amo A, González-de-laAleja P, Boix V, Gil J: Post-acute COVID-19 syndrome: incidence and risk factors: a Mediterranean cohort study. *J Infect* 2021, 82: 378–383
43. Henkin RI, Larson AL, Powell RD: Hypogeusia, dysgeusia, hyposmia, and dysosmia following influenza-like infection. *Ann Otol Rhinol Laryngol* 1975, 84:672–682